Mateusz Sowa

Effect of Welding Parameters on the Strength of Safety Cages

Abstract: Safety cages, constituting essential equipment in sports car, aim to reduce consequences of potential accidents. These structures should provide the highest possible and reproducible level of workmanship aimed to ensure their strength as that assumed at the design stage. Because of the fact that welding is the primary technology used in the fabrication of safety cages it is highly necessary to analyse the effect of welding parameters as well as the choice of welding methods on process repeatability and strength properties of welded joints. The aim of this study was to determine the influence of the welding method on the strength of test cruciform joints of tubes as well as to investigate the effect resulting from the change of MAG and TIG welding current parameters on the linear deformation of welded joints. The article discusses the effect of welding process conditions on the static strength of cruciform joints in steel E355 +N (used in the fabrication of safety cages). The tests revealed that an increase in heat input during welding significantly reduced the strength of cruciform joints as well as significantly contributed to an increase in post-weld linear deformation, which, in terms of spatial safety of cage structure, could lead to a significant pile-up of stresses.

Key words: automotive industry, safety cell, testing of welded joints, safety cages, welding, racing sports, roll cages, motorsport

DOI: 10.32730/mswt.2024.68.1.5

1. Introduction

Depending on their category, sports car bodies are divided into two basic types. Category I cars are based on car bodies from series production, yet are suitably reinforced for use in motor sport. In turn, category II cars have dedicated bodies, e.g. having the form of carbon-fibre monocoques as in Formula 1 or WEC cars, or the form of space tube structure, used in T-group cars from the 2022 Rally season.

Safety cages are some of the most essential elements affecting the safety of motorsport competitors. These structures increase the rigidity of the bodywork, contributing to greater control of the vehicle during cornering and are also key elements of the vehicle responsible for passive safety, reducing the effect of body deformation during a crash. The roll cage is a spatial tubular structure connected to the car body tasked (in the event of collision with an obstacle or during rollover) with the distribution of impact forces evenly among various components of the structure. The primary purpose of the roll cage is to cushion the impact and protect the driver and pilot. An exemplary safety cage installed in the car body is presented in Figure 1.

Fig. 1. Safety cage [11]

2. Test pieces

The research work involved the performance of technological welding tests using sections of cold-drawn seamless tubes made of steel E355 + N (ϕ45.0 × 2.5 mm) in accordance with PN-EN 10305-1:2010 [1]. The tests were preceded by the check analysis concerning the chemical composition of the test pieces (Table 1). The analysis was performed using a Q4 Tasman spark excitation emission spectrometer (Bruker).

Table 1. Chemical composition of the test steel grade and normative requirements for contents of alloying elements in steel E355 + N.

Table 1. Chemical composition of the test steel grade and normative requirements for contents of alloying elements in steel E355 + N

Chemical composition	Alloying element, wt.%							
	C	Mn	Si	P	S	Cr	Mo	Ni
Analysis	0.17	1.38	0.22	0.013	0.006	0.011	0.042	0.015
PN-EN 10305-1	max. 0.22	max. 1.60	max. 0.55	max. 0.25	max. 0.015	–	–	–

mgr inż. Mateusz Sowa – Łukasiewicz Research Network – Upper-Silesian Institute of Technology, Welding Centre, Research Group for Materials Weldability and Welded Structures
Corresponding author: mateusz.sowa@git.lukasiewicz.gov.pl

3. Welding consumables

The test pieces were welded using an UltraMag solid copper electrode wire (Lincoln Electric) designated as G 46 5 M 4Si1 (in accordance with PN-EN ISO 14341-A) [2]. The shielding gas used in the process was the M21-ArC-18 gas mixture (in accordance with PN-EN ISO 14175).

4. Welding process and test results

The model test joints presented in Fig. 1a were made from previously prepared tubular sections, milled to a radius corresponding to the diameter of the base tube (in order to accurately match the edges to be welded). Sharp edges of the test pieces were subjected to grinding aimed at the removal of a material overhang resulting from the machining of the test pieces (Figure 2b).

The research-related tests were focused on one type of welded joint used in safety cage structures. The reason for the aforesaid choice was the highest welding repeatability and the possibility of conducting strength tests (static tensile tests). Exemplary tubular cruciform joints used in automotive safety cages are presented in Fig. 3.

The research work involved the performance of technological welding tests as well as visual and macroscopic examinations of the test joints. The results obtained in the tests were used to develop four technologies enabling the making of tubular cruciform joints. The three of the aforesaid technologies were based on the MAG method, whereas one was based on the TIG method. The welding parameters of the test joints subjected to further tests are presented in Table 2.

Each of the technologies presented in the Table 2 was used to make four tubular cruciform (a total of 16 joints). The making of the joints was followed by measurements of tube deformations. The results of the measurements are presented in Table 3.

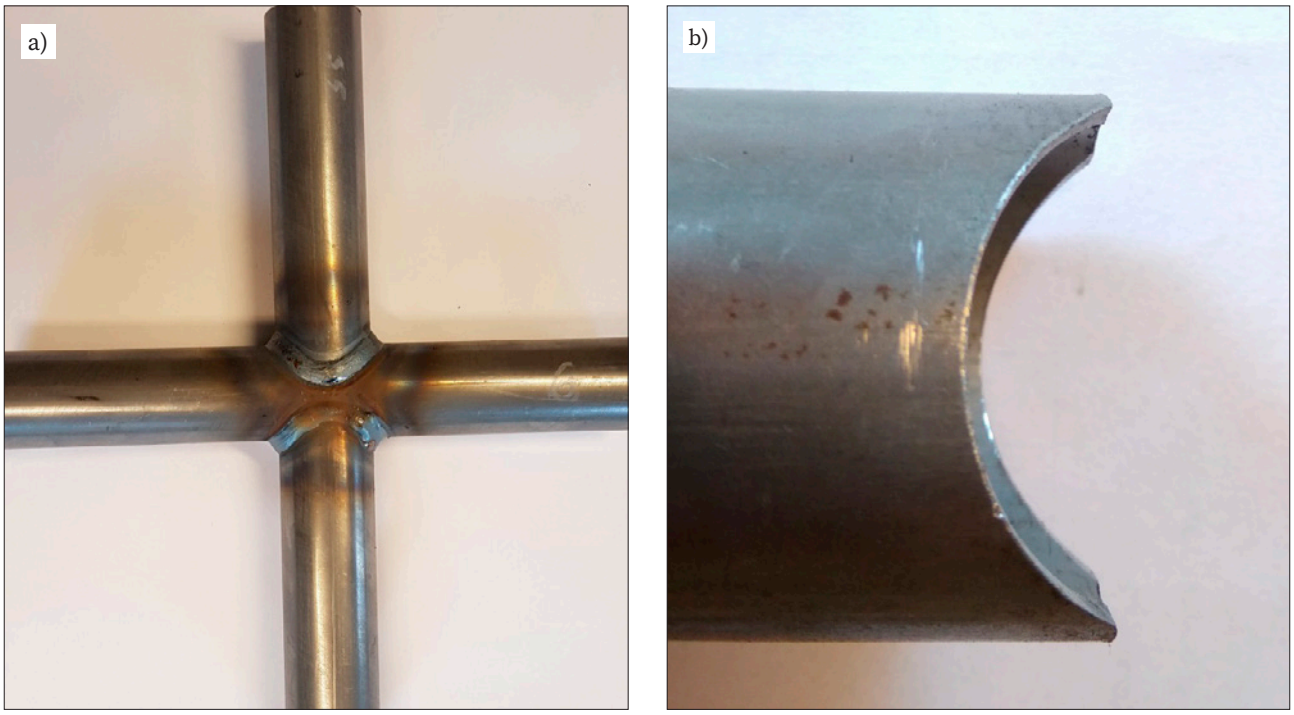

Fig. 2. Model joint subjected to the tests (a) and the pre-weld preparation of the components (b)

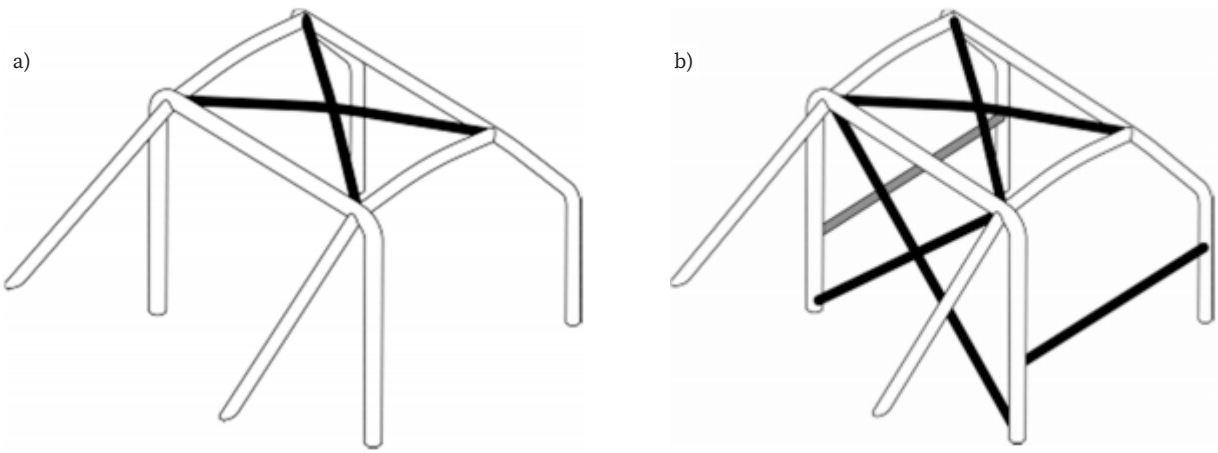

Fig. 3. Examples of cruciform joints used in automotive safety cages [3]

Table 2. Welding process parameters

Test joint no.	Welding method	Filler metal wire diameter [mm]	Current [A]	Arc voltage [V]	Type of current/ polarity	Filler metal wire feed rate [m/min]	Welding rate [cm/min]	Heat input [kJ/mm]
1	135	1.0	135	18	DC (+)	5	31.2	0.389
2	135	1.0	150	20	DC (+)	6	31.2	0.450
3	135	1.0	100	17.8	DC (+)	3.5	31.2	0.348
4	141	2.4	110	13	DC (-)	-	7.2	0.715

Table 3. Results of post-weld measurements of longitudinal deformations

Test joint	longitudinal deformation [mm]				
	Joint no. 4.1	Joint no. 4.2	Złącze próbne 4.3	Joint no. 4.4	Average
1	-0.5	-0.6	-0.5	-0.5	-0.525
2	-1.4	-1.2	-1.2	-1.3	-1.3
3	-0.4	-0.3	-0.3	-0.3	-0.325
4	-1.4	-1.4	-1.3	-1.5	-1.4

Table 4. Static tensile test results

Specimen no.	S_o, mm^2	F_m, kN	R_m, MPa	Remarks
1.1	333.6	172.2	516.1	rupture took place in the welded tube (beam) material transversely to the tensile axis
1.2	333.6	174.3	522.6	rupture took place in the welded tube (beam) material transversely to the tensile axis
2.1	333.6	157.2	471.1	rupture took place in the welded tube (beam) material transversely to the tensile axis
2.2	333.6	158.6	475.3	rupture took place in the welded tube (beam) material transversely to the tensile axis
3.1	333.6	174.1	522.0	rupture took place in the welded tube (beam) material transversely to the tensile axis
3.2	333.6	175.6	526.3	rupture took place in the welded tube (beam) material transversely to the tensile axis
4.1	333.6	142.2	426.1	rupture took place in the weld
4.2	333.6	130.0	389.7	rupture took place in the weld
Symbols	S_o – initial cross-sectional area of the specimen [mm^2], F_m – force at rupture [kN], R_m – stress at rupture [MPa]			

4.1 Static tensile tests

The subsequent stage included the performance of static tensile tests. The tensile tests involved two welded joints made using the previously-developed welding technologies. The results of the static tensile tests are presented in Table 4.

The results of the static tensile tests revealed that all the MAG welded joints (test joints 1, 2 and 3) subjected to the tensile tests failed, where the tube split transversely to the tensile axis. Welded joints 2.1 and 2.2, in relation to which the highest heat input technology was used, revealed lower tensile strength compared to that of the other joints welded using this method. The results of the static tensile test concerning the TIG-welded test joints revealed that the tensile strength of these joints was by about 100 MPa lower than that of the MAG-welded joints. The difference at the point of rupture was also significant as, unlike in terms of the MAG-welded test joints, the TIG-welded joints ruptured in the weld. Photographs of the test joints after the static tensile test are presented in Figure 4.

4.2 Macroscopic metallographic tests

Macroscopic metallographic tests involved metallographic specimens sampled from the areas marked in Figure 5. Each test joint was sampled for four metallographic specimens.

The macroscopic metallographic examinations revealed welding imperfections (incomplete fusion) in test joints nos. 2 and 4. Test joint no. 4 was characterised by incomplete fusion, fillet weld misalignment and burn-through.

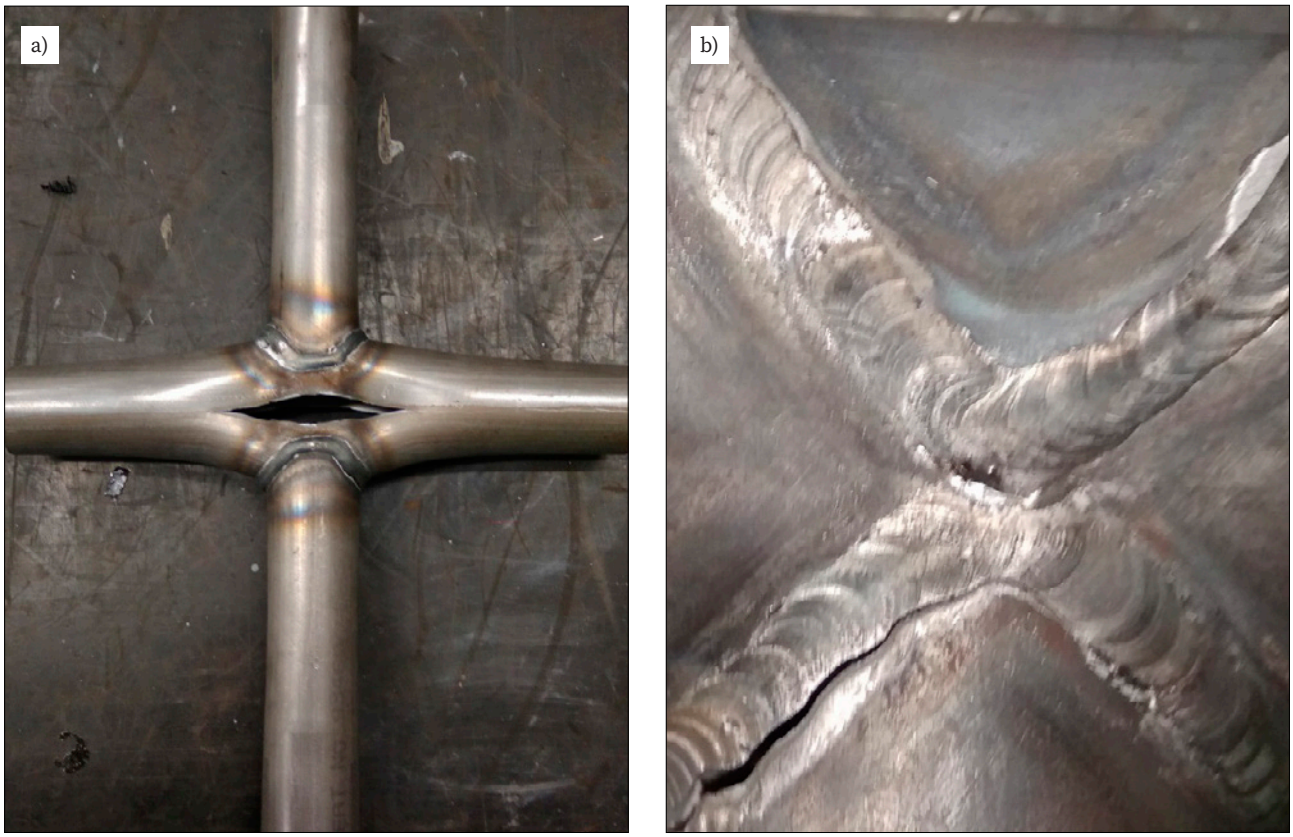

Fig. 4. a) MAG-welded specimen after the tensile test and b) TIG weld after the tensile test

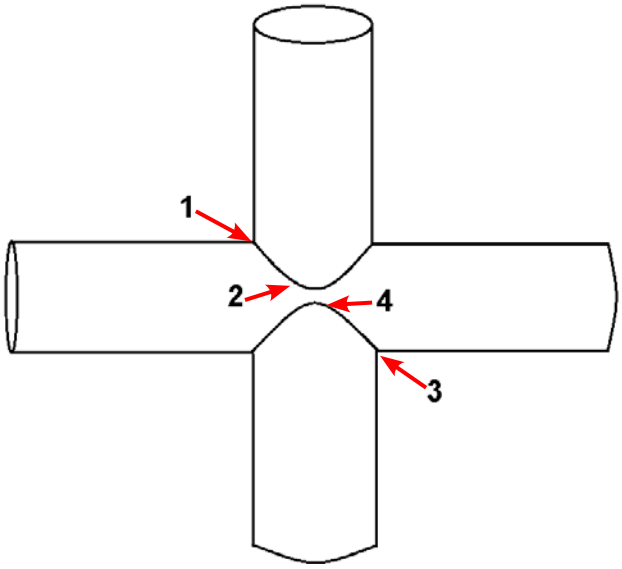

Fig. 5. Areas sampled for metallographic specimens; the macroscopic metallographic test results are presented in Figs. 6–9

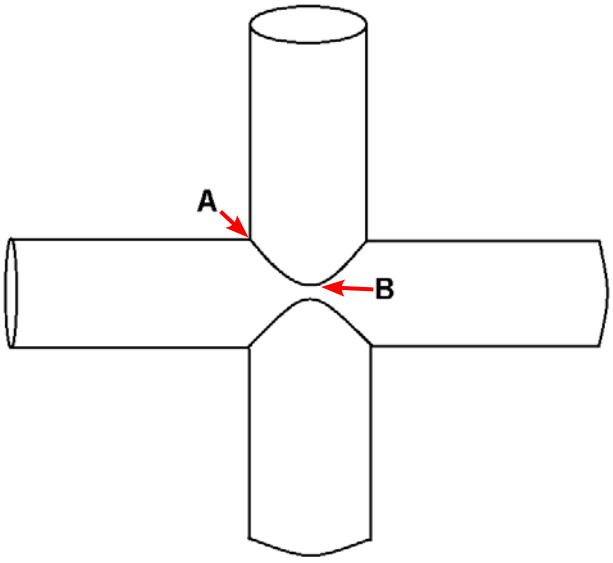

Figure 10: Areas subjected to the hardness test

4.3. Hardness measurements

Hardness measurements, based on the Vickers hardness test, were performed under a load of 98.7 N. The parent material, heat affected zone (HAZ) and the weld were subjected to three measurements performed in accordance with the schematic diagram presented in Table 5. The tests, involving all areas of the joints, were performed using a KB50-BYZ-FA hardness tester (KB Prüftechnik). The locations of the areas subjected to the hardness tests are presented in Figure 10.

The test results did not reveal any unfavourable increase in hardness above a limit value of 380 HV10. All the hardness measurement results were restricted within the range of 151 HV10 to 272 HV10.

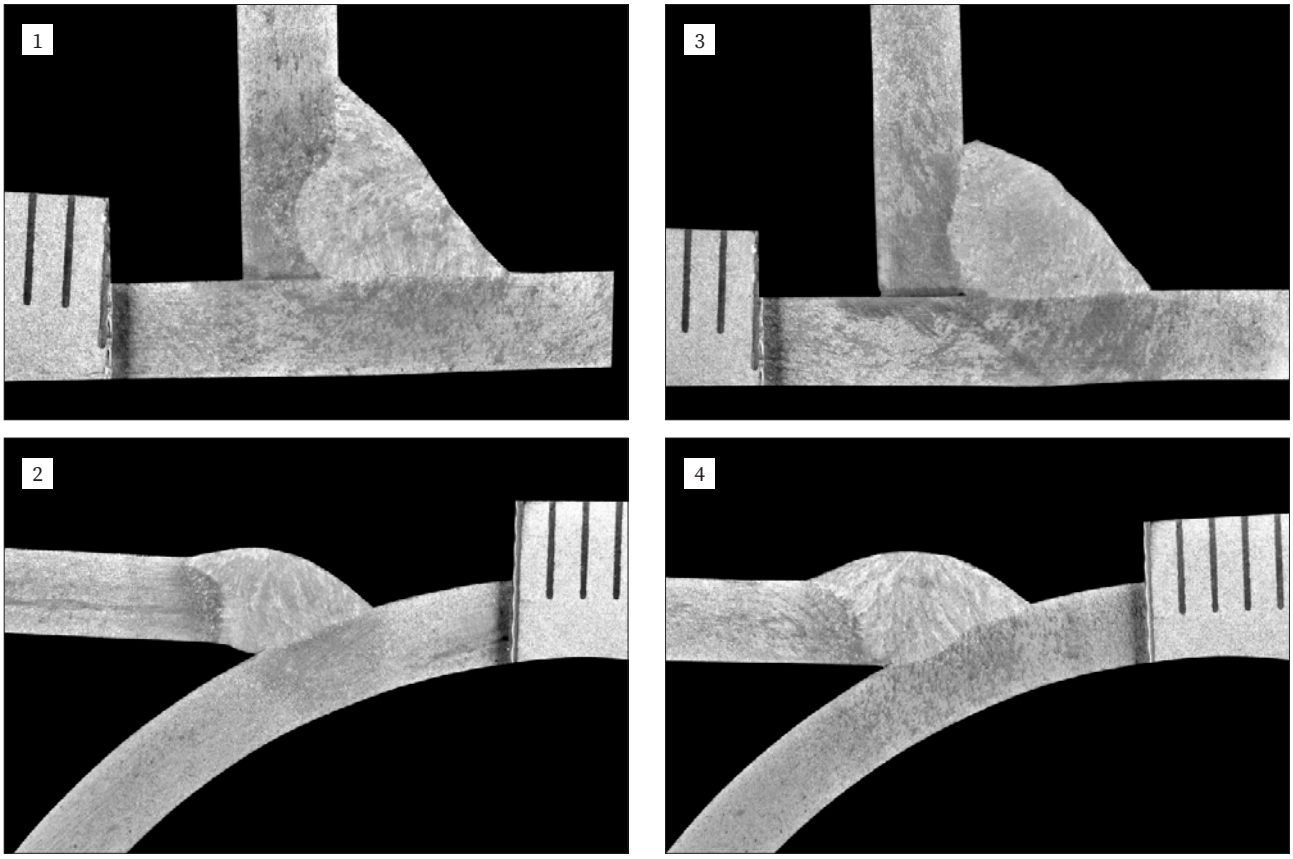

Fig. 6. Macroscopic test results of test joint no. 1 (in accordance with the diagram in Fig. 5)

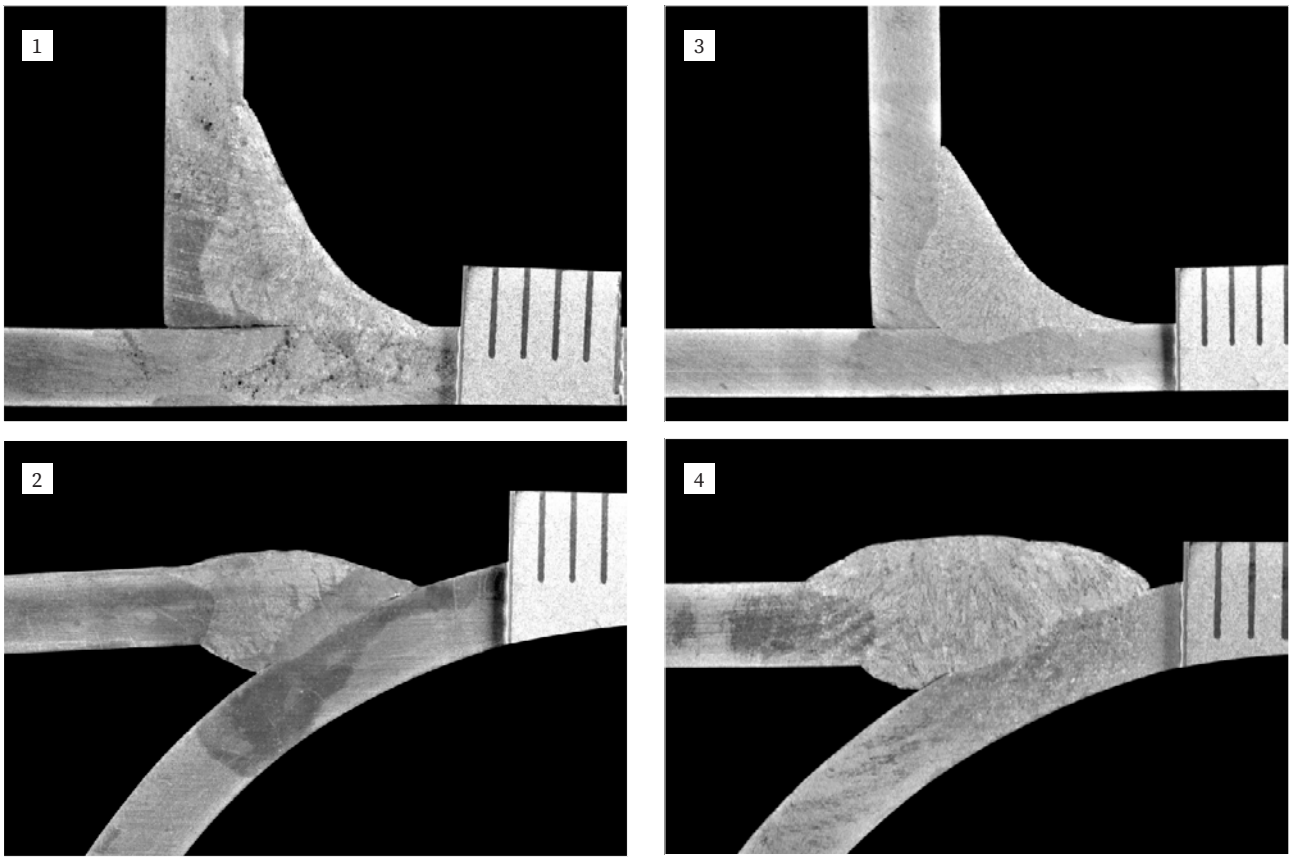

Fig. 7. Macroscopic test results of test joint no. 2

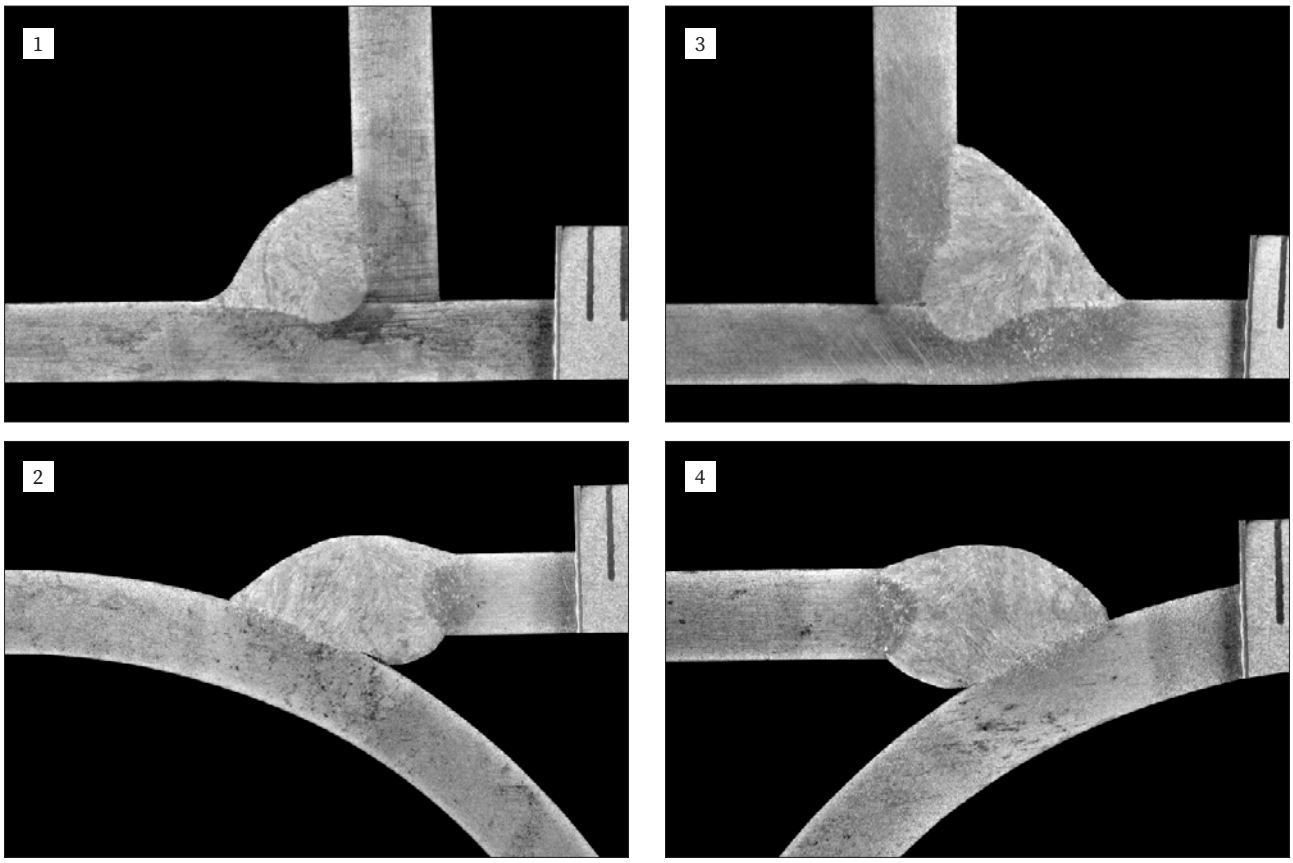

Fig. 8. Macroscopic test results of test joint no. 3

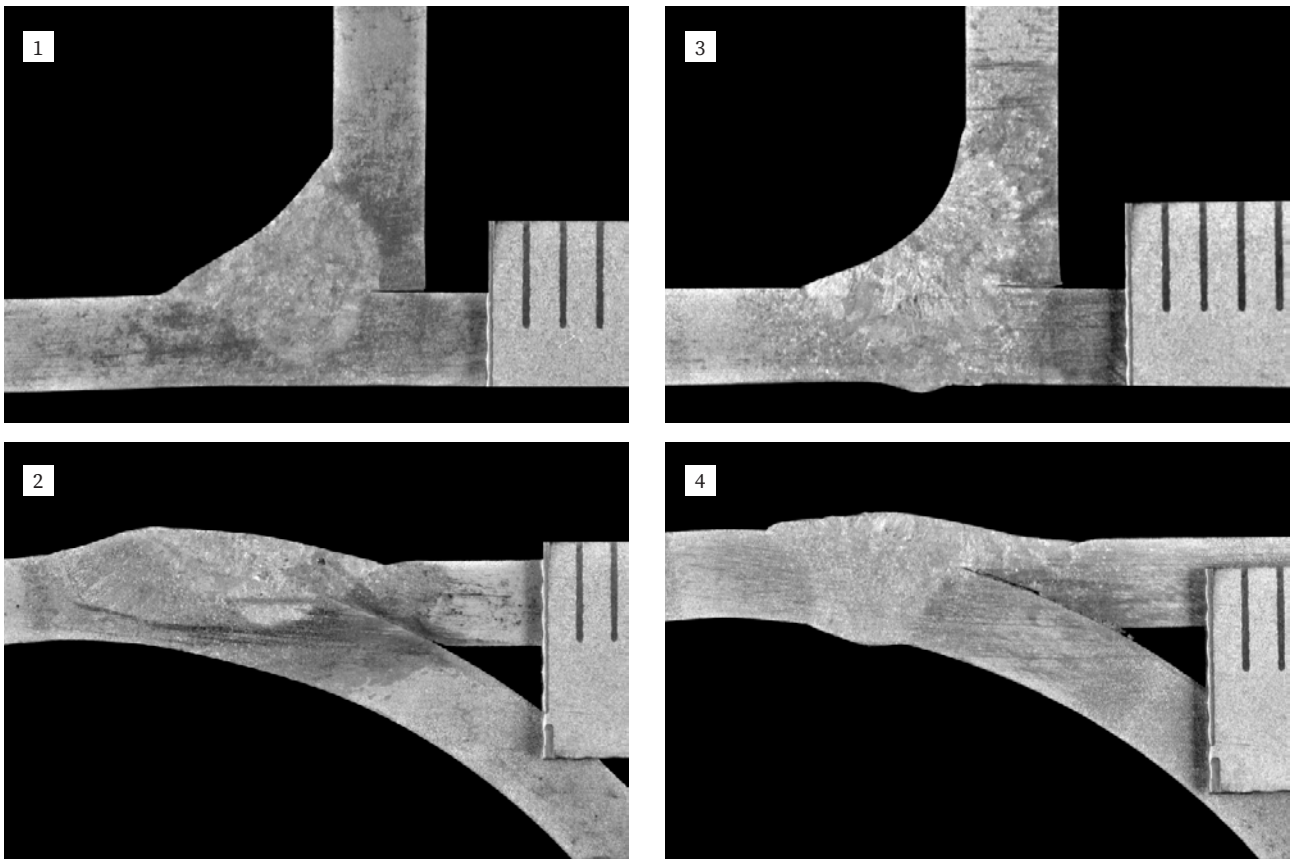

Fig. 9. Macroscopic test results of test joint no. 4

Table 5. Results of the hardness tests in the area of the angle joint

Specimen no.	Test line	Place of measurement and hardness (HV10):														
		Base material			HAZ 1			Weld			HAZ 2			Base material		
		1	2	3	4	5	6	7	8	9	10	11	12	13	14	15
4	A	162	169	165	218	223	231	191	201	197	221	241	239	156	171	151
	B	161	161	166	231	219	239	222	212	211	231	247	261	158	156	151
6	A	155	155	172	206	208	217	193	184	181	202	207	204	154	152	153
	B	166	158	160	221	219	230	215	213	213	249	252	269	151	153	154
7	A	160	164	175	228	220	240	197	200	197	228	244	232	152	152	152
	B	182	179	175	217	256	236	211	209	206	245	266	272	155	155	149
8	A	177	178	185	247	242	234	198	197	210	224	234	215	171	160	158
	B	157	160	167	205	200	197	218	222	209	203	189	194	176	167	164

Arrangement of the measurement points

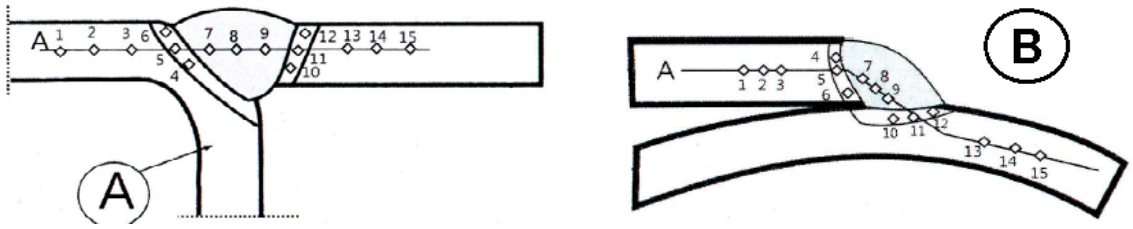

5. Conclusions

1. The study revealed that increased current parameters and fillet weld thickness in cruciform joints resulted in the reduction of strength properties by up to 20 % (approximately 100 MPa). One reason for the above-named phenomenon could be attributed to the necessity of increasing the welding rate in order to avoid excess weld metal and overlaps, resulting in the lack of penetration in the base material.
2. The tests also revealed that an increase in linear energy during the making of tubular cruciform joints was accompanied by an almost three-fold increase in the linear deformation, which, when welding the entire safety cage, could significantly weaken the welded structure, generating stresses in the structural nodes.
3. Welded joints of safety cage structures are special and problematic types of joints, including both T-joints with fillet welds in one area (where components intersect) and overlap joints with fillets welds.

REFERENCES:

[1] PN-EN 10305-1:2016. Rury stalowe precyzyjne – Warunki techniczne dostawy – Część 1: Rury bez szwu ciągnione na zimno

[2] PN-EN ISO 14341:2011 „Materiały dodatkowe do spawania – druty elektrodowe i stopiwo do spawania łukowego elektrodą metalową w osłonie gazu stali niestopowych i drobnoziarnistych – klasyfikacja"

[3] Art. 253 – Wyposażenie bezpieczeństwa (Grupa N, A, R-GT), Załącznik „J" – MKS FIA.

[4] Alghamdi A. A. A.: Collapsible impact energy absorbers: an overview. Thin-Walled Structures, Elsevier 2001, vol. 39, pp. 189–213.

[5] Kotełko M., Lipa S.: Model teoretyczny i doświadczalny absorbera energii poddanego zgniotowi bocznemu. Czasopismo techniczne. Wydawnictwo Politechniki Krakowskiej im. Tadeusza Kościuszki, January 2006. pp. 195–205.

[6] Pawłowski J.: Nadwozia samochodowe, wyd.3. Wydawnictwa Komunikacji i Łączności, Warszawa 1978.

[7] Alexander J. M.: An approximate analysis of the collapse of thin cylindrical shells under axial loading. The Quarterly Journal of Mechanics and Applied Mathematics, 1960, vol. 13, 1, pp. 10–15.

[8] Kotełko M.: Nośność i mechanizmy zniszczenia konstrukcji cienkościennych, Wydawnictwo Wydawnictwa Naukowo-Techniczne, Warszawa 2011.

[9] Lipa S.: Koncepcja bezpiecznego samochodu. Praca magisterska. Politechnika Łódzka 2002.

[10] https://www.quora.com/What-cars-never-had-sway-bars-under-the-chassis-for-side-stabilization

[11] Dangarh A , Kulkarni V., Katarne R. and Sharma M. Structural Analysis of an ATV Frame. International Journal of Scientific and Research Publications, 2015, vol. 5.

[12] Harvir Singh, Mayank K.: Design and optimization of an All-Terrain Vehicle roll cage IOP Conf. Ser.: Mater. Sci. Eng. 1149 012021.

[13] Penugula D. R. R, Naresh C., Phanisankar B. S. S.: Design and structural analysis of baja frame with conventional and composite materials. International Journal Of Advance Scientific Research and Engineering Trends, 2020, vol. 5, pp. 23–31.

[14] Soundararajan R. et al.: A novel approach for design and analysis of an all-terrain vehicle roll cage. Materials Today: Proceedings, 2020, vol. 45, pp. 2239–2247.

[15] Saplinova V., Novikov I., Glagolev S.: Design and specifications of racing car chassis as passive safety feature. Transportation Research Procedia, 2020, no. 50, pp. 591–607.